ORIGINAL RESEARCH

Adenosine diphosphate-decorated chitosan nanoparticles shorten blood clotting times, influencing the structures and varying the mechanical properties of the clots

Tze-Wen Chung[1,3]
Pei-Yi Lin[2]
Shoei-Shen Wang[2]
Yen-Fung Chen[3]

[1]Department of Biomedical Engineering, National Yang-Ming University, [2]Department of Surgery, National Taiwan University Hospital, Taipei, Taiwan, Republic of China; [3]Department of Chemical and Materials Engineering, National Yunlin University of Science and Technology, Yunlin, Taiwan, Republic of China

Correspondence: Tze-Wen Chung
No.155, Sec. 2, Linong St. Taipei, 112, Taiwan, Republic of China
Email twchung@ym.edu.tw

Shoei-Shen Wang
No. 1, Jen Ai Road, Section 1, Tapei, 100 Taiwan, Republic of China
Email wangp@ntu.edu.tw

Abstract: Chitosan nanoparticles (NPs) decorated with adenosine diphosphate (ADP) (ANPs) or fibrinogen (FNPs) were used to fabricate hemostatic NPs that can shorten blood clotting time and prevent severe local hemorrhage. The structure and mechanical properties of the blood clot induced with ANP (clot/ANP) or FNP (clot/FNP) were also investigated. The NPs, ANPs, and FNPs, which had particle sizes of 245.1 ± 14.0, 251.0 ± 9.8, and 326.5 ± 14.5 nm and zeta potentials of 24.1 ± 0.5, 20.6 ± 1.9, and 15.3 ± 1.5 mV (n=4), respectively, were fabricated by ionic gelation and then decorated with ADP and fibrinogen. The zeta potentials and Fourier transform infrared (FTIR) spectroscopy of the NPs confirmed that their surfaces were successfully coated with ADP and fibrinogen. The scanning electron microscope (SEM) micrographs of the structure of the clot induced with "undecorated" chitosan NPs (clot/NP), clot/ANP, and clot/FNP (at 0.05 wt%) were different, after citrated bloods had been recalcified by a calcium chloride solution containing NPs, ANPs, or FNPs. This indicated that many NPs adhered on the membrane surfaces of red blood cells, that ANPs induced many platelet aggregates, and that FNPs were incorporated into the fibrin network in the clots. Measurements of the blood clotting times (Tc) of blood clot/NPs, clot/ANPs, and clot/FNPs, based on 90% of ultimate frequency shifts measured on a quartz crystal microbalance (QCM), were significantly ($P<0.05$) (n=4) shorter than that of a clot induced by a phosphate-buffered solution (PBS) (clot/PBS) ($63.6\% \pm 3.1\%$, $48.3\% \pm 6.2\%$, and $63.2\% \pm 4.7\%$, respectively). The ΔF_2 values in the spectra of frequency shifts associated with the propagation of fibrin networks in the clot/ANPs and clot/FNPs were significantly lower than those of clot/PBS. Interestingly, texture profile analysis of the compressional properties showed significantly lower hardness and compressibility in clot/NPs and clot/ANPs ($P<0.05$ or better) (n=4) compared with clot/PBS and clot/FNPs. Accordingly, among the hemostatic NPs, ANP substantially reduced blood clotting times, ΔF_2 values, and compression flow properties of the clot. Hence, ANPs have potential applications for preventing severe local hemorrhage.

Keywords: hemostatic NPs, ADP, fibrinogen, compressional properties

Introduction

Preventing severe hemorrhage is essential for reducing mortality and improving survival in emergencies or other medical events, such as severe trauma.[1,2] Hemostatic biomaterials reduce or stop bleeding by accelerating blood clot formation, and they must be biocompatible and must have low toxicity. Of the commercially available hemostats, the HemCon® chitosan (CS) bandage (HemCon Medical Technologies, Inc., Portland, OR, USA) and QuikClot® zeolite powder (Z-Medica Corp, Wallingford, CT, USA) are reportedly the most effective for reducing or stopping bleeding. The former comprises a lyophilized CS derivate, with positively charged amine groups, which accelerate blood

clot formation by attracting negatively charged molecules or proteins on red blood cell (RBC) membranes or in plasma (eg, fibrinogen).[3,4] The latter absorbs water released from injured sites and can increase local platelet concentrations and coagulation factors.[5,6] The chemical reactions of QuikClot zeolite powder are exothermic, and the powder has poor biodegradability. Therefore, it can injure tissues, such as blood vessels. This powder is also less biocompatible than CS and other natural biomaterials.[7] However, neither product can actively trigger the constituents of the blood coagulation pathway in the hemostatic process. The blood coagulation pathway can be actively triggered by incorporating blood coagulation molecules (eg, fibrinogen) on substrate surfaces, which stops bleeding by accelerating the formation of blood clots, and is worthy of investigation.

Owing to its nontoxicity and high bioactivity, CS, an amino polysaccharide (poly 1, 4-D-glucoamine), is widely used for drug delivery and for engineering tissues, such as for osteogenesis or cardiomyogenesis from mesenchymal stem cells.[8–10] Additionally, CS nanoparticles (NPs) exhibit a positive potential in buffer solutions because of the protonization of their amine groups. This effect is often exploited to deliver proteins such as insulin or deoxyribonucleic acid (DNA) to specific cells.[11,12] In a recent study of a CS sponge treated with sodium hydroxide to accelerate blood clotting, its hemostatic efficacy was comparable with that of commercial CS bandages. Adsorbed plasma proteins (eg, fibrinogen) and extracellular matrix proteins (eg, collagen) can promote platelet adhesion on the surfaces of CS nanoparticles. This effect, which is mainly mediated by αIIbβ3 and α2β1 integrins, rapidly stops bleeding.[13] Hence, decorating CS with plasma proteins, such as fibrinogen, may accelerate blood clotting and reduce bleeding, while influencing the structures and mechanical properties of clots. However, to the best knowledge of the authors, no studies have reported the use of CS NPs decorated with fibrinogen (FNPs).

Adenosine diphosphate (ADP) is an important physiological agonist that has a crucial role in normal hemostasis and thrombosis. ADP is well known to activate platelets through three receptors: P2Y1 and P2Y12, which are G protein–coupled receptors, and P2X1, a ligand-gated ion channel receptor. The P2Y1 receptor is important in changing the shapes of platelets as well as in their aggregation, thromboxane A2 generation, adhesion to immobilized fibrinogen, and thrombus formation under shear conditions. The second ADP receptor, the P2Y12 receptor, reportedly has important roles in platelet functions, very much like the P2Y1 receptor. Furthermore, the P2Y12 receptor also participates in platelet activations mediated by other physiological agonists, including collagen.[14] Hence, ADP-decorated CS NPs (ANPs) may accelerate blood clotting by activating platelets and influence the structure and mechanical properties of clots. However, the fabrication of ANPs for investigation of the aforementioned issues has not been evaluated.

Fibrinogen is a plasma glycoprotein with a high molecular weight (approximately 340 kDa) and a normal blood plasma concentration of 200–400 mg/dL (2–4 g/L). In the blood coagulation pathway, thrombin usually cleaves fibrinogen to form fibrin segments, which polymerize to form a fibrin network. The fibrin network entraps the constituents of blood, including blood cells and platelets, forming blood clots that are stabilized by activated factor XIII.[15] Fibrinogen in the blood plasma is important in platelet adhesion because it can bind to the platelet glycoprotein IIb/IIIa receptor.[16] It has also been shown that the adhesion of platelets onto FNPs is mainly mediated by glycoprotein IIb/IIIa ligand/receptor interactions; at the same time, the configuration of the fibrinogen might be influenced by the CS and consequently unable to activate platelets in suspensions determined by P-selectin expression.[13] However, the effects of FNPs on the rate of blood clot formation and clot structure have not been fully investigated.

This study recalcified freshly citrated blood samples in phosphate-buffered solution (PBS) containing "undecorated" CS NPs, ANPs, and FNPs to investigate whether these hemostatic nanoparticles could accelerate blood clotting. Scanning electron microscope (SEM) (JSM-6700F, JEOL Co., Tokyo, Japan) micrographs of the clots were examined to investigate the interactions among clot components, such as the fibrin network, platelets, and the various NPs. The blood clotting times (Tc) of clots induced by the various NPs were measured with a quartz crystal microbalance (QCM). The QCM has demonstrated high sensitivity to small changes in mass, such as changes caused by the absorption of a protein on a surface or blood coagulation/clot formation, to which the oscillation frequency of the quartz in the device responds.[17–21] The oscillation frequency shifts (ΔF_2) associated with the propagation of the fibrin network during the formation of clots were analyzed to determine how ANPs or FNPs affect blood clot structure. Compressional flow properties, including clot hardness and compressibility, were determined by texture profile analysis[22–24] using a micromechanical test system. This study investigated the effects of adding "undecorated" CS NPs, ANP and FNP on the rates of blood clot formation, on blood clot structure, and on compressional flow properties, to evaluate their potential use for preventing severe local hemorrhage.

Materials and methods
Materials
CS (low molecular weight, 75%–85% deacetylated), acetic acid, ADP, and fibrinogen were purchased from Sigma-Aldrich Corp (St Louis, MO, USA). Sodium citrate was obtained from Nacalai Tesque, Inc., (Kyoto, Japan). Phosphotungstic acid was purchased from Thermo Fisher Scientific Inc (Waltham, MA, USA).

Preparing CS NPs, ANPs, and FNPs
To prepare the CS solution, 0.1 g of CS was dissolved in 100 mL of 1% acetic acid solution. To fabricate CS NPs, 500 mL of CS solution was stirred at 420 rpm at 4°C; 8 mL of sodium citrate solution (50 mg/mL) was then injected into the CS solution using a syringe pump with a flow rate of 12 mL/hr, and the solution was further stirred for 30 minutes. The CS NP suspension was centrifuged at 25,000 g, for 12 minutes at 4°C, to separate the NPs from the suspension, and the NPs were collected. The NPs were washed three times with deionized water, centrifuged (which gently removed water from the surfaces of the NPs), and dried under vacuum at room temperature.[25,26] For the blood clotting study, dried NPs were resuspended in PBS with mild stirring, at a finite concentration.

The ANPs were prepared by using a syringe pump (flow rate 12 mL/hr) to inject ADP solution (2,550 μM) into the CS NP suspension, which was then stirred at 100 rpm at 4°C for 30 minutes to stabilize the coating process. The same procedures used for the CS NP preparation were used to separate and then dry the ANPs.[25,26]

The FNPs were prepared by injecting fibrinogen solution (0.1 mg/mL) into the CS NP suspension using a syringe pump, with a flow rate of 12 mL/hr, which was then stirred at 100 rpm at 4°C for 30 minutes to stabilize the coating process. The same procedures used for the CS NP preparation were used to separate and then dry the FNPs.[25,26]

Characterizations of the various NPs by particle size, zeta potential, TEM, and ATR-FTIR spectra
The size and zeta potential of various NPs in aqueous solution was determined at 25°C using a dynamic light scattering analyzer equipped with zeta potential measurement, measured by a 5 mW laser (90Plus Zeta; Brookhaven Instruments Corp, Holtsville, NY, USA) (λ=633 nm). The procedures are described in detail elsewhere.[25] The morphology of the NPs was observed by transmission electron microscopy (TEM) (JEOL 1200EX; JEOL Ltd, Tokyo, Japan) as described elsewhere.[25] Briefly, the NP solution

was placed on a 300 mesh copper grid coated with carbon. The NPs on the copper grid were then stained with 2.0 wt% of phosphotungstic acid. After air drying at room temperature, the morphology of the stained NPs was observed and imaged using the TEM. The attenuated total reflectance Fourier transform infrared (ATR-FTIR) spectra of various NPs were detected at a resolution of 2 cm⁻¹ with a ATR-FTIR spectrum analyzer (Spectrum One NTS; PerkinElmer Inc., Waltham, MA, USA) and analyzed using a built-in standard software package. Briefly, 50 mg of the dried NPs was mixed with potassium bromide (KBr) and punched to a pellet for measuring their spectra. The detailed procedures are described elsewhere.[25,26]

SEM morphologies of blood clots without and with added hemostatic NPs
The study protocol was approved by the Institutional Review Board at National Taiwan University hospital before the initiation of the study. Written informed consent was obtained from the healthy blood donors. Fresh blood was initially mixed with a sodium citrate buffer (10:1 by volume) containing 0.9% NaCl and 0.15% $CaCl_2$ at pH 6. The blood was centrifuged at 1,200 g for 10 minutes to adjust its hematocrit (Hct) to 45%. The adjusted blood was recalcified by adding $CaCl_2$ solution containing 0.1 mL of various hemostatic NPs and then mixing gently.[27] Owing to dilution effects, the blood samples were activated at final concentrations of 0.05% NPs and 0.40% Ca^{+2} with a Hct of 38%, to form clots. The morphology of the blood clots induced with or without NPs (in PBS solution) addition was observed by SEM (JSM-6700F, JEOL Co., Tokyo, Japan), using a procedure described elsewhere.[26,27]

The QCM for determining blood Tc and ΔF_2 of clots
A 0.5 mL quantity of the Hct-adjusted blood, at final concentrations of 0.05% NPs and 0.40% Ca^{+2}, was dropped onto a 9 MHz gold electrode on the QCM (ADS; ANT Technology Co, Ltd, Taipei, Taiwan, Republic of China) at 37°C. The frequency of the QCM response to the weight changes on the electrode and clot formation was then monitored continuously.[17,21] The frequency spectra of the clot formations in QCM measurements can be found elsewhere.[17] According to an earlier investigation,[17] the Tc values should be taken when the frequency has shifted by 90% of the ultimate ΔF_2 in response to clot formation. The ΔF_2 of clots was obtained by calculating the differences in frequency during propagation of the fibrin network.[17]

Determining the compressional flow properties (hardness and compressibility) of blood clots by texture profile analysis (TPA)

Clots, induced by various NP samples, of 2 cm in height and 3 cm in diameter were formed in sample bottles, at 37°C. The clots samples were stabilized at 37°C for more than 20 minutes. The mechanical properties of the various clot samples were evaluated using a Micromechanical Test System (model CY6101A1; Chun Yen Testing Machines Co. Ltd., Taichung, Taiwan, Republic of China), in a TPA mode. A tubular probe (10/150 mm, diameter/length) was inserted twice into each sample, to a depth of 15 mm, at a rate of 120 mm/min, with a 15-second delay between insertions, according to the techniques of TPA.[22–24] Hardness and compressibility of the tested samples were determined by calculating the areas of the spectra of the TPA measurements.[22–24]

Measuring blood viscosity during clot formation

A cone/plate viscometer (model LVTDV-II; Brookfield Engineering Laboratories, Inc., Middleboro, MA, USA) with cone angle of 0.80 was utilized to continuously measure the viscosity of the recalcified bloods during the coagulation process, at 37°C with the shear rate of 12 sec^{-1}, until the clots were fully formed.[26] The viscosity curve during blood clot formation was measured and was similar to that of an earlier report.[26] The curve was utilized to calculate the viscosity changes for blood clotting.

Statistical analysis

All calculations used the Systat® SigmaStat® statistical software (version 9) (Jandel Scientific Software Corp., San Rafael, CA, USA). Statistical significance was evaluated at a 95% confidence level or better. Data are presented as mean ± standard deviation for n=3 or 4 measurements.

Results and discussion
Characterizations of hemostatic nanoparticles
### Morphologies of CS NPs, ANPs, and FNPs

Figure 1A–C presents the TEM morphologies of the CS NPs, ANPs, and FNPs. Interestingly, the FNPs had a core–shell type morphology (Figure 1C) and were larger than the CS NPs and ANPs, consisting of CS NP cores with a surface coating of fibrinogen molecules. Since the molecular weight of ADP is low, TEM could not clearly reveal the surface coating of the ANPs (Figure 1A and B). The laser scattering particle analyzer revealed that the sizes of the CS NPs, ANPs, and FNPs were
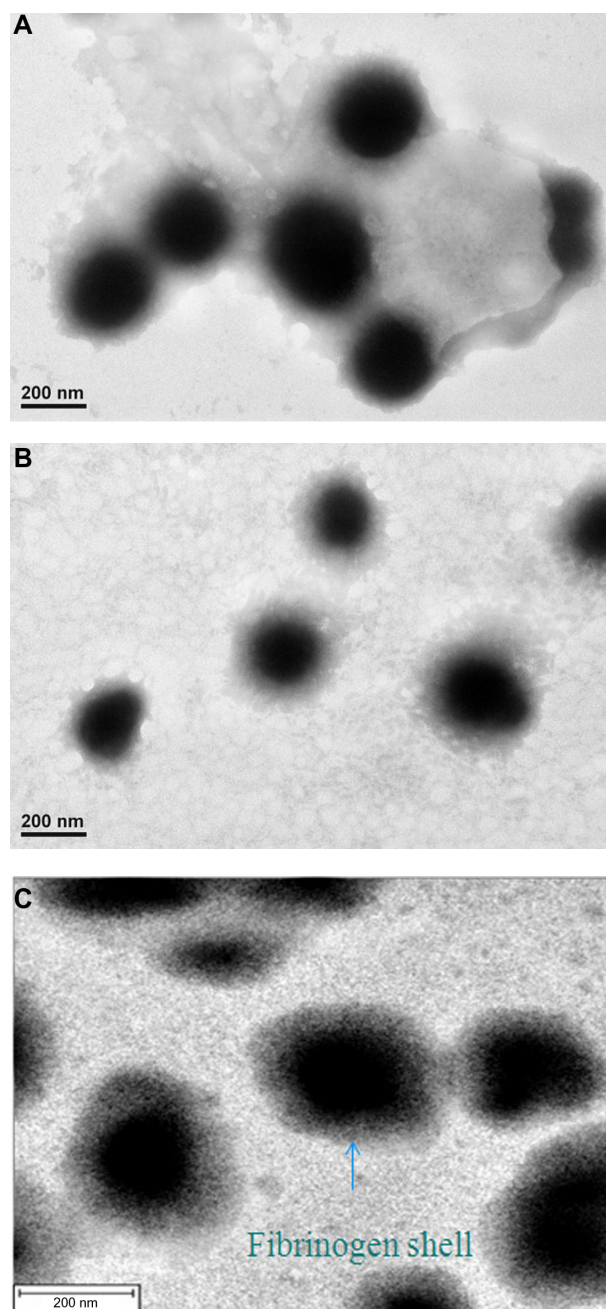
Figure 1 The TEM micrographs of (**A**) CS NPs, (**B**) ANPs, and (**C**) FNPs, showing solid spheres with a shielding fibrinogen shell (150K× or deleted).
Abbreviations: ADP, adenosine diphosphate; ANP, ADP-decorated CS NP; CS NP, chitosan nanoparticle; FNP, fibrinogen-decorated CS NP; TEM, transmission electron microscopy.

245.1±14.0, 251.0±9.8, and 326.5±14.5 nm, respectively. The FNPs (n=4) were significantly larger ($P<0.01$) than the CS NPs or ANPs, which was consistent with the morphology observed by TEM. The zeta potentials of the CS NPs, ANPs, and FNPs were 24.1±0.5, 20.6±1.9, and 15.3±1.5 mV (n=4), respectively, which revealed that the negative charges of the fibrinogen molecules on the surface coatings of the CS NPs significantly reduced ($P<0.05$) (n=4) their zeta potentials.[8,9] To confirm
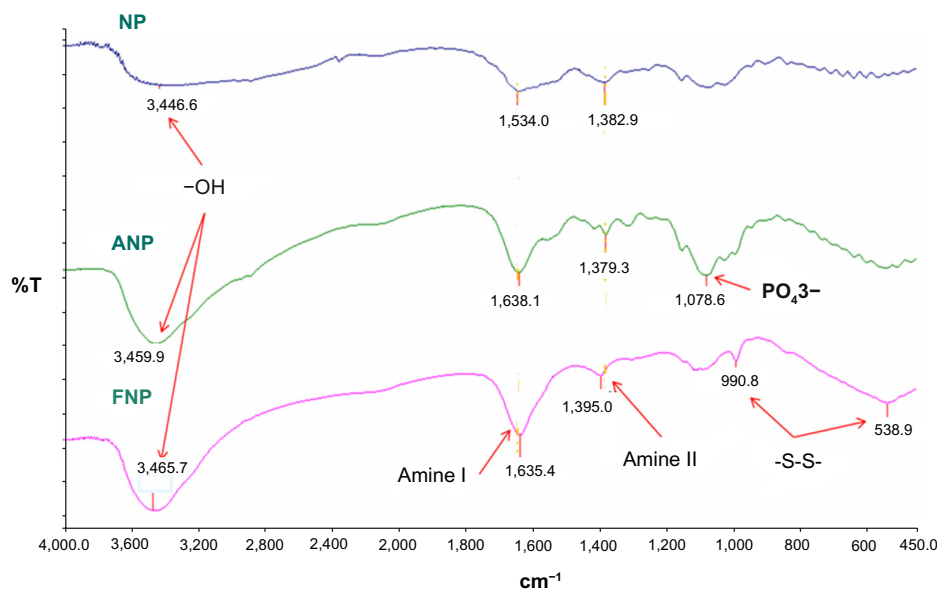
Figure 2 The ATR-FTIR transmission spectra of CS NPs, ANPs, and FNPs.
Notes: The spectra of NPs are shown for amide I (1,638 cm⁻¹) of CS. The characteristic peaks for ADP and fibrinogen on NP surfaces are also shown, respectively.
Abbreviations: ADP, adenosine diphosphate; ATR-FTIR, attenuated total reflectance Fourier transform infrared spectroscopy; ANP, ADP-decorated CS NP; CS NP, chitosan nanoparticle; FNP, fibrinogen-decorated CS NP; NP, nanoparticle.

the presence of ADP and fibrinogen on the NP surfaces, FTIR spectra were obtained for the three NPs (Figure 2). The absorption peaks for the CS in the NPs included those at 1,383 and 1,638 cm⁻¹ for amides II and I, respectively, and a broad peak at 3,346–3,465 cm⁻¹ for the OH⁻ group.[8–10] The ANPs and FNPs yielded the same peaks, with shifts in the case of FNPs that were produced by fibrinogen molecules. The ANPs and FNPs revealed absorption peaks at 1,079 cm⁻¹ for PO⁻³ and at 991 cm⁻¹ and 539 cm⁻¹ for the S–S (disulfide bonds) in the fibrinogen peptides,[19] respectively (Figure 2), which confirmed that the NPs were decorated with ADP and fibrinogen. Comparisons of zeta potentials and absorption peaks in the FTIR spectra of the ANPs and FNPs with those of the CS NPs further confirmed the successful coating of the CS NPs with ADP and fibrinogen, respectively. Although earlier studies have prepared FNPs to study platelet activation,[13] fibrinogen decoration on CS NPs has not been demonstrated as clearly as in this study.

Hemostatic NPs for reduced blood Tc
Morphology of blood clots

Microscope analysis of the clot induced in PBS solution, namely, clot/PBS, and the clot induced by the various NPs (data not shown) showed that their morphologies were similar to those reported in an earlier study that was carried out in this laboratory.[27] However, the initial Hct (45%) of the blood samples was reduced to around 38% in the clots in this study, which were lower than that in the clots reported in an earlier study[25,27] because of the addition of NPs to induce the samples to clot. Notably, in the earlier study, blood with a Hct of 45% was used to test the thrombolysis capability of drug-loaded NPs,[25,27] while, in this study, the Hct of 38% was used, to mimic the local hemorrhage/hemostatic NP conditions when clots would be initiated to prevent severe hemorrhage. Figure 3A presents a typical SEM micrograph of a blood clot formed by the aggregation of RBCs, platelets, and fibrin networks, although the fibrin networks were relatively smaller than those formed at normal Hct (about 41%) since the Hct of the clot was low. The SEM micrograph of the clot induced by the CS NP solution (clot/NP) in Figure 3B differs from that in Figure 3A. Although RBC aggregates and platelets in both Figure 3A and B were distributed throughout the clot, many of the CS NPs adhered to the membrane of the RBCs in Figure 3B, but not in 3A. Since CS was a constituent of all the NPs and had a positive zeta potential, CS interacted with the negative charges on the RBC membrane during clot formation. Notably, the SEM micrograph of the clot induced by the ANP solution (clot/ANP) (Figure 3C) shows many more aggregates of platelets compared with the clots in Figure 3A and B. The formation of the platelet aggregates in Figure 3C may have resulted from ADP on the ANP surfaces, which simultaneously activated many platelets during clot formations.[14] The activation of platelets by ANPs is one of the objectives in the design of the ANPs. The SEM micrograph of the clot induced by the FNP solution (clot/FNP) (Figure 3D) demonstrates that the fibrin network in the clot/FNP had a much higher density than the fibrin network in clot/NP (Figure 3B) or clot/ANP (Figure 3C). Some fibrin networks were bridged
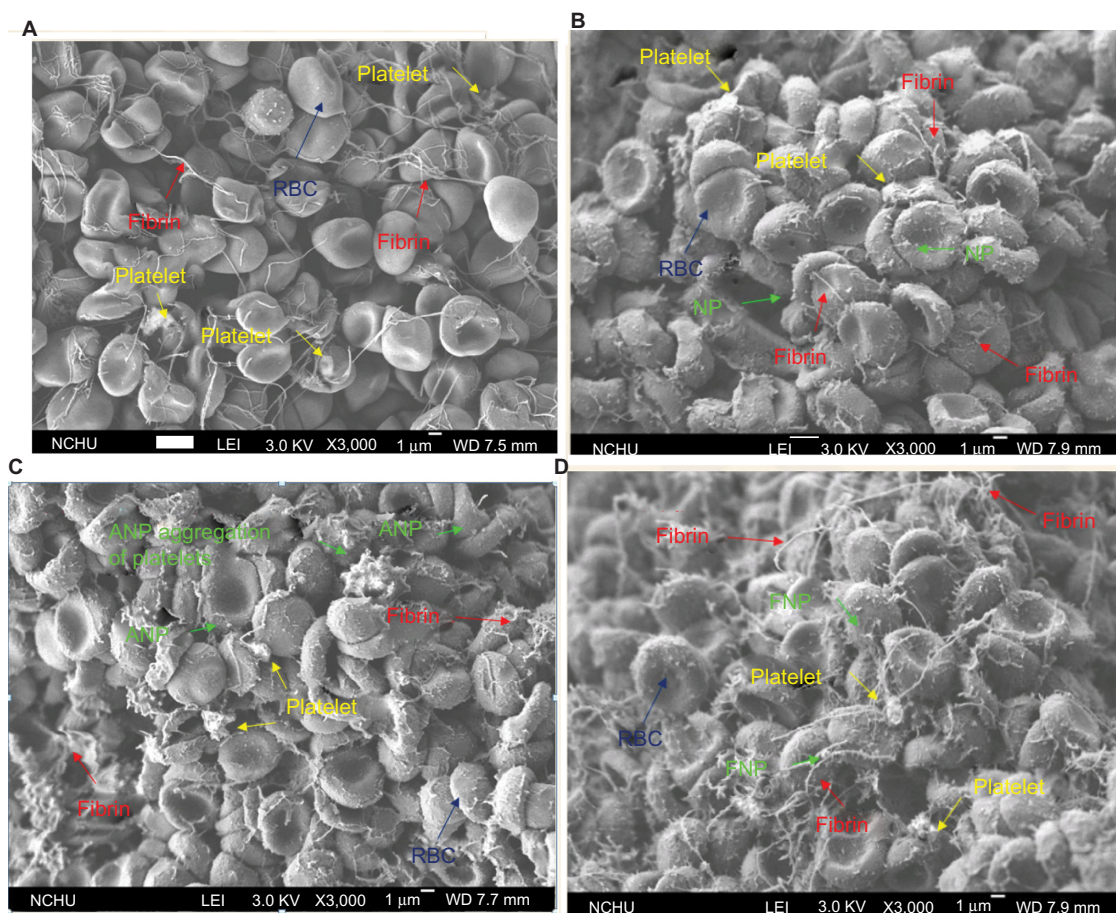
Figure 3 SEM micrographs of (**A**) clot/PBS showing the RBC aggregates, platelets, and fibrin network; (**B**) clot/NP showing many CS NPs adhering to the surfaces of RBCs or RBC aggregates; (**C**) clot/ANP showing many platelet aggregates in the clot; and (**D**) clot/FNP showing many FNPs adhering to the RBCs or RBC aggregates.
Note: In (**D**), the fibrin network is also much denser than that in other clots (**B** and **C**).
**Abbreviations:** ANP, adenosine diphosphate–decorated chitosan nanoparticle; Clot/ANP, clot induced in ANP solution; Clot/FNP, clot induced in FNP solution; Clot/NP, clot induced in CS NP solution; Clot/PBS, clot induced in phosphate-buffered solution; CS NP, chitosan nanoparticle; FNP, fibrinogen-decorated chitosan nanoparticle; RBC, red blood cell; SEM, scanning electron microscopy.

by FNPs (Figure 3D) in the clot/FNP but not in other clots (Figure 3A–C). We hypothesize that thrombin in the blood sample simultaneously activated fibrinogen molecules on the surfaces of many FNPs and in the blood. These molecules then facilitated construction of fibrin networks of clot/FNP, which potentially accelerated clot formation, as described below. The morphology of some of the RBC cells in the clots (Figure 3) were transformed to spheres after forming clots, possibly due to the interactions of the CS-based NPs and RBC cells during the clotting process or to the sample preparations for the SEM study. However, this did not affect the objectives of this study, ie, stopping severe local hemorrhage or enhancing clot formation, and did not reveal the toxicity of NPs to RBCs.

Blood Tc was reduced by hemostatic NPs evaluated by measuring frequency shift of a QCM

The Tc values of the clot/PBS and clot/NP, clot/ANP, and clot/FNP were obtained with a QCM and a conventional CCD

recorder (Sony XC-500 digital video camera module, Sony Corporation, Tokyo, Japan). The QCM has been extensively utilized for measuring small changes in mass. Protein adsorption and cell adhesion on quartz crystals result in ΔF_2.[17,18,21] As measured on a QCM, a clot formation reportedly produces a continuous ΔF_2. This phenomenon provides a sensitive and convenient method for measuring the Tc values of clots.[17,19] Figure 4 plots a typical response curve of the ΔF_2 measured by the QCM during clot formation, which is similar to curves presented elsewhere.[17,21] Briefly, recalcified blood samples containing the various NPs were loaded onto a QCM sensor, which rapidly reduced its frequency, by approximately 4KHz, within approximately 30 seconds. Although blood coagulation may have begun in this period, stable clots were later detected, at approximately 200 seconds, after which a stably oscillating ΔF_2 was observed (Figure 4A). According to an earlier investigation, the Tc values should be taken when the frequency has shifted by 90% of the ultimate frequency

A

B

C

D
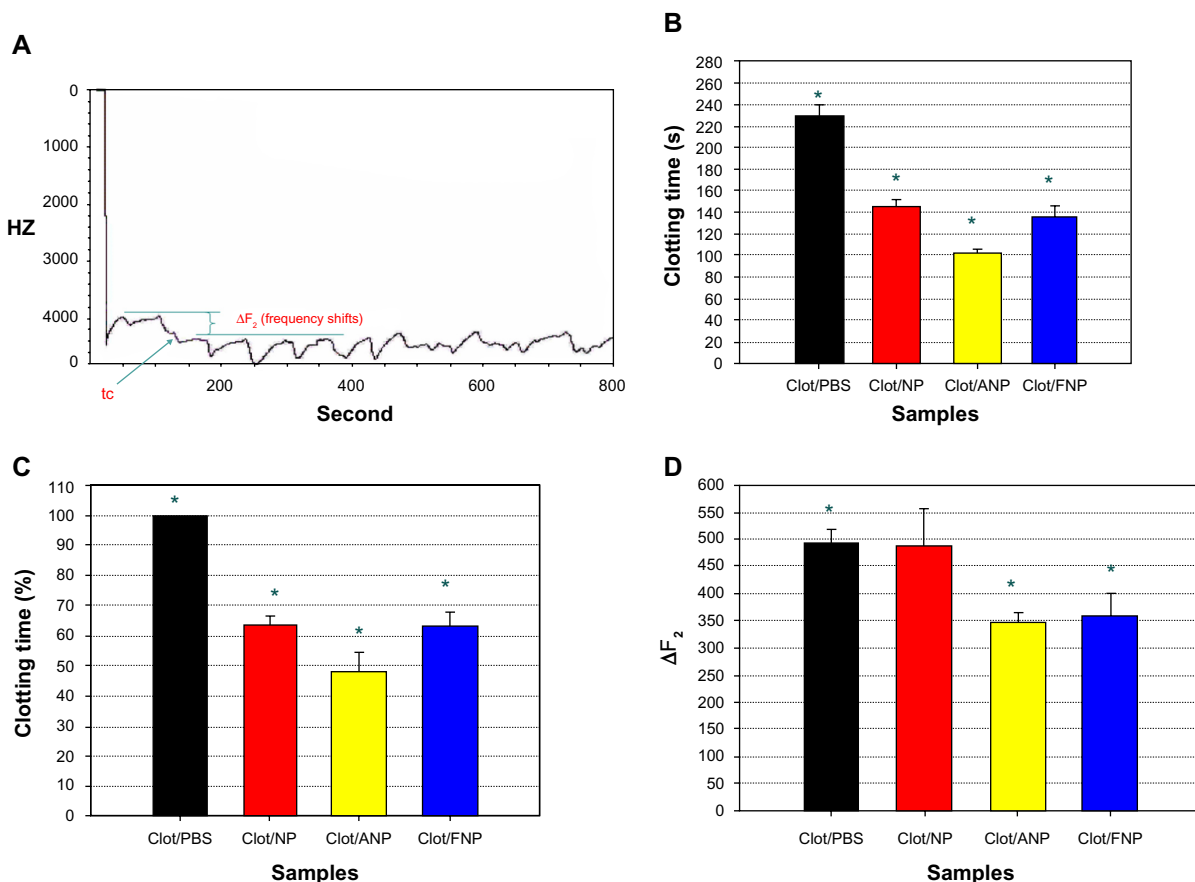
Figure 4 (**A**) Typical frequency shifts of QCM in response to recalcified blood containing the various NPs. (**B**) The Tc values of clots induced by the various NPs. The Tc values of clot/NP, clot/ANP, and clot/FNP were significantly lower than that of clot/PBS. (**C**) The reductions (%) of the Tc values for clots induced by various CS NPs compared with that of clot/PBS. (**D**) The ΔF_2 values for clot/NP, clot/ANP, and clot/FNP. The ΔF_2 values for clot/ANP and clot/FNP were significantly lower than for the others (*$P<0.05$ or better).

Notes: The Tc value was taken when the 90% of the ultimate frequency shift of QCM response. The ΔF_2 of clots was obtained by calculating during propagation of the fibrin network.

Abbreviations: ΔF_2, frequency shift; ANP, adenosine diphosphate–decorated chitosan nanoparticle; Clot/ANP, clot induced in ANP solution; Clot/FNP, clot induced in FNP solution; Clot/NP, clot induced in CS NP solution; Clot/PBS, clot induced in phosphate-buffered solution; CS NP, chitosan nanoparticle; FNP, fibrinogen-decorated chitosan nanoparticle; NP, nanoparticle; QCM, quartz crystal microbalance; Tc, clotting time; s, second.

shift, in response to clot formation.[17] The same approach was used to determine Tc values herein (Figure 4A). Notably, the Tc values of the blood clot/NP, clot/ANP, and clot/FNP (Figure 4B) were significantly shorter (63.6%±3.1%, 48.3%±6.2%, and 63.2%±4.7%, respectively) (n=4) ($P<0.01$) than that of the clot/PBS (229.5±9.5 seconds) (Figure 4C). The Tc values measured by the QCM were similar to those obtained directly from the frames of a recording of dynamic clotting captured using the CCD recorder (Table 1). The results in Figure 4B indicate that adding hemostatic NPs to blood accelerated blood clotting and reduced the Tc. The clotting spectrum obtained by the QCM was further analyzed to compare the shift in ΔF_2 among various clot/NP, clot/ANP, and clot/FNP (Figure 4D). The ΔF_2 value for the clot/PBS did not differ from that of clot/NP. Interestingly, however, the ΔF_2 values of clot/ANP and clot/FNP were significantly lower than that of clot/NP (Figure 4D). The variation in ΔF_2

values may have resulted from different interior structures of the clots. The period over which ΔF_2 was measured was the stage of the blood clot process at which the fibrin network propagates,[17] which would be influenced by the viscosity and density of the clot, as described by the equation derived by Kanazawa and Gordon.[28] Interestingly, the ΔF_2 values obtained in this study were similar to those revealed by the oscillatory circuit in the QCM with dissipation monitoring (QCM-D) technique, which is used to detect mass deposition or changes in the viscosity of adjacent liquids or blood clots on quartz sensors.[17,19] Although the energy dissipation attributable to the differences in viscosity and density among the clot/PBS and others could not be evaluated by this QCM system, the SEM morphologies of the clots analyzed herein indicated the variation in ΔF_2 values among clots. The SEM morphologies in Figure 3 and the long Tc values (Figure 4B and C) indicate that the fibrin network in clot/PBS, which was only activated

Table 1 The Tc values of clots tested were measured with a conventional CCD recorder

| Clot type	Tc value ± SD (sec)
Clot/PBS	210.80±2.56*
Clot/NP	131.00±2.80*
Clot/ANP	93.67±2.19*
Clot/FNP	128.00±6.08*

Notes: The Tc values of clots with various CS NPs were significantly lower than that of clot/PBS, while that of clot/ANP was the lowest. The CCD recorder and QCM showed similar trends in Tc values. (*$P<0.05$ or better) (n=4).
Abbreviations: ANP, adenosine diphosphate–decorated chitosan nanoparticle; CCD, charge-coupled device; CS NP, chitosan nanoparticle; Clot/ANP, clot induced in ANP solution; Clot/FNP, clot induced in FNP solution; Clot/NP, clot induced in CS NP solution; Clot/PBS, clot induced in phosphate-buffered solution; CS NP, chitosan nanoparticle; FNP, fibrinogen-decorated chitosan nanoparticle; PBS, phosphate-buffered solution; QCM, quartz crystal microbalance; SD, standard deviation; Tc, clotting time.

by $CaCl_2$ solution, had a long propagation time; its network of relatively densely connected and aggregated RBCs increased the viscosity of the clot/PBS, to approximately 2.56 times the viscosity of the blood sample. This increase was above that of the clot/FNP and clot/ANP, which were approximately 1.70 and 1.66 times the viscosity of the blood samples (n=3), respectively. Hence, the ΔF_2 of the clot/PBS exceeded that for the clot/FNP and that for the clot/ANP (Figure 4D), according to the equation of Kanazawa and Gordon.[28] The increased viscosity of the clots might explain the similar ΔF_2 for the clot/NP and clot/PBS since the increase in the viscosity of the clot/NP (a factor of 2.44 times) over that of the blood sample was approximately the same as that measured for the clot/PBS. However, the role of the changes in density of the clots containing various NPs needs further study.

Compression flow properties of clots with hemostatic NPs

In analyses of the shear flow properties of blood clots, a thromboelastograph has been used to determine their viscoelastic properties and their strength by other investigators.[29] The compressional flow properties of gels, such as hardness and compressibility, are frequently determined by TPA;[22–24] these methods can also be used to elucidate the properties of blood clots. Hardness refers to the force required to deform a gel, and it is related to viscosity.[22,23] Polymeric entanglements increase the hardness and compressibility of gels, which then increase their resistance to deformation. In contrast, a low hardness indicates that a gel can be easily employed at the site of hemorrhage.[22,24] Interestingly, the hardness of the clot/NP or clot/ANP was significantly lower ($P<0.05$) than that of the clot/PBS (Figure 5A). However, the hardness of the clot/FNP was similar to that of the clot/PBS. Compressibility or spreadability govern the deformation of gels when they are first compressed by a probe[22,23] and quantifies the ease of spreading a gel on a site. A gel with low compressibility can be easily spread over the desired site. The compressibility/spreadability of the blood clots varied in a manner similar to hardness (Figure 5B). Hence, the entanglements of the fibrin network with RBCs in clot/PBS and clot/FNPs (Figure 3A and D) were greater than those of clot/NPs and clot/ANPs (Figure 3B and C), but clot/NPs and clot/ANPs are probably more easily spread over injured sites compared with the other two types of clot (Figure 5B). This study is the first to describe how hemostatic nanoparticles affect the hardness and compression in blood clots.
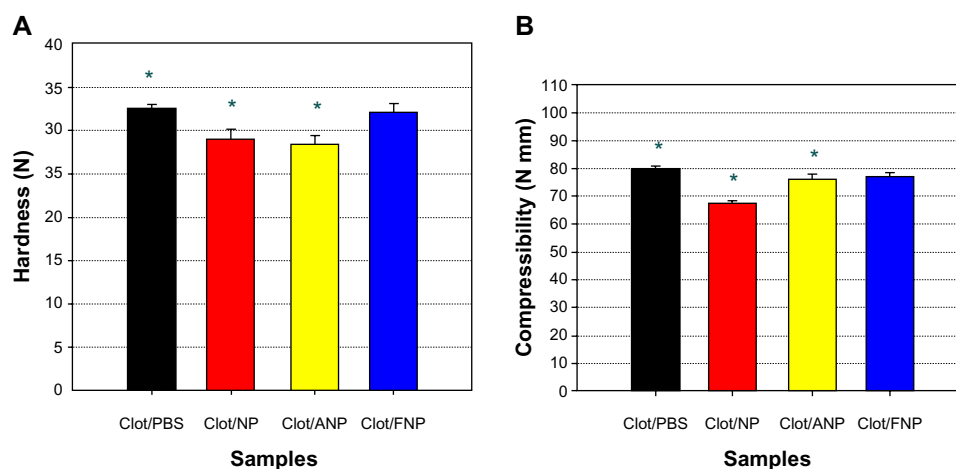
Figure 5 (**A**) The hardness of various clots was examined by TPA analysis. Hardness values of clot/NP and clot/ANP were lower than others, indicating the former was easily deformed. (**B**) The compressibility of various clots was presented. Compressibility values of clot/NP and clot/ANP were lower than others, indicating the former was easily spread over the desired site.
Abbreviations: ANP, adenosine diphosphate–decorated chitosan nanoparticle; Clot/ANP, clot induced in ANP solution; Clot/FNP, clot induced in FNP solution; Clot/NP, clot induced in CS NP solution; Clot/PBS, clot induced in phosphate-buffered solution; CS NP, chitosan nanoparticle; FNP, fibrinogen-decorated chitosan nanoparticle; TPA, texture profile analysis.

Conclusion

Hemostatic CH NPs, ANPs, and FNPs were fabricated, with particle sizes of 245.1±14.0, 251.0±9.8, and 326.5±14.5 nm (n=4), and zeta potentials of 24.1±0.5, 20.6±1.9, and 15.3±1.5 mV (n=4), respectively. Blood clots induced with 0.05 wt% ANPs in recalcified blood solutions had larger decreases in Tc values (eg, 48.3%±6.2% [n=4]) compared with those induced with clot/NPs, clot/FNPs, and clot/PBS. Clot/ANPs, clot/NPs, and clot/FNPs influenced the structures of blood clots. The ΔF_2 value of clot/ANP was significantly lower than those of clot/PBS and clot/NP. Additionally, the hardness and compressibility of clot/ANPs were significantly lower than those of clot/FNPs and clot/PBS. In conclusion, hemostatic ANPs have strong potential for preventing severe hemorrhage in medical events.

Acknowledgments

Disclosure

Reference

1. Dai C, Liu C, Wei J, Hong H, Zhao Q. Molecular imprinted macroporous chitosan coated mesoporous silica xerogels for hemorrhage control. *Biomaterials*. 2010;31(30):7620–7630.
2. Ward KR, Tiba MH, Holbert WH, et al. Comparison of a new hemostatic agent to current combat hemostatic agents in a Swine model of lethal extremity arterial hemorrhage. *J Trauma*. 2007;63(2):276–283; discussion 283–284.
3. Kozen BG, Kircher SJ, Henao J, Godinez FS, Johnson AS. An alternative hemostatic dressing: comparison of CELOX, HemCon, and QuikClot. *Acad Emerg Med*. 2008;15(1):74–81.
4. Gu R, Sun W, Zhou H, et al. The performance of a fly-larva shell-derived chitosan sponge as an absorbable surgical hemostatic agent. *Biomaterials*. 2010;31(6):1270–1277.
5. Ahuja N, Ostomel TA, Rhee P, et al. Testing of modified zeolite hemostatic dressings in a large animal model of lethal groin injury. *J Trauma*. 2006;61(6):1312–1320.
6. Rhee P, Brown C, Martin M, et al. QuikClot use in trauma for hemorrhage control: case series of 103 documented uses. *J Trauma*. 2008;64(4): 1093–1099.
7. Seyednejad H, Imani M, Jamieson T, Seifalian AM. Topical haemostatic agents. *Br J Surg*. 2008;95(10):1197–1225.
8. Yang MC, Wang SS, Chou NK, et al. The cardiomyogenic differentiation of rat mesenchymal stem cells on silk fibroin-polysaccharide cardiac patches in vitro. *Biomaterials*. 2009;30(22):3757–3765.
9. Muzzarelli RAA. Chitosan composites with inorganics, morphogenetic proteins and stem cells, for bone regeneration. *Carbohydr Polym*. 2011;83(4):1433–1445.
10. Chi NH, Yang MC, Chung TW, Chou NK, Wang SS. Cardiac repair using chitosan-hyaluronan/silk fibroin patches in a rat heart model with myocardial infarction. *Carbohydr Polym*. 2013;92(1):591–597.
11. Xu Q, Guo L, Gu X, et al. Prevention of colorectal cancer liver metastasis by exploiting liver immunity via chitosan-TPP/nanoparticles formulated with IL-12. *Biomaterials*. 2012;33(15):3909–3918.
12. Liao ZX, Peng SF, Ho YC, Mi FL, Maiti B, Sung HW. Mechanistic study of transfection of chitosan/DNA complexes coated by anionic poly(γ-glutamic acid). *Biomaterials*. 2012;33(11):3306–3315.
13. Lord MS, Cheng B, McCarthy SJ, Jung M, Whitelock JM. The modulation of platelet adhesion and activation by chitosan through plasma and extracellular matrix proteins. *Biomaterials*. 2011;32(28):6655–6662.
14. Falker K, Lange D, Presek P. P2Y12 ADP receptor-dependent tyrosine phosphorylation of proteins of 27 and 31 kDa in thrombin-stimulated human platelets. *Thromb Haemost*. 2005;93(5):880–888.
15. Guyton AC, Hall JE. *Textbook of Medical Physiology*. 2005, 11th edition, WB Saunders Co., Philadelphia, USA.
16. Tsai WB, Grunkemeier JM, McFarland CD, Horbett TA. Platelet adhesion to polystyrene-based surfaces preadsorbed with plasmas selectively depleted in fibrinogen, fibronectin, vitronectin, or von Willebrand's factor. *J Biomed Mater Res*. 2002;60(3):348–359.
17. Cheng TJ, Chang HC, Lin TM. A piezoelectric quartz crystal sensor for the determination of coagulation time in plasma and whole blood. *Biosens Bioelectron*. 1998;13(2):147–156.
18. Thierry B, Winnik FM, Merhi Y, Tabrizian M. Nanocoatings onto arteries via layer-by-layer deposition: toward the in vivo repair of damaged blood vessels. *J Am Chem Soc*. 2003;125(25):7494–7495.
19. Müller L, Sinn S, Drechsel H, et al. Investigation of prothrombin time in human whole-blood samples with a quartz crystal biosensor. *Anal Chem*. 2010;82(2):658–663.
20. Sperling C, Fischer M, Maitz MF, Werner C. Blood coagulation on biomaterials requires the combination of distinct activation processes. *Biomaterials*. 2009;30(27):4447–4456.
21. Yang MH, Jong SB, Lu CY, et al. Assessing the responses of cellular proteins induced by hyaluronic acid-modified surfaces utilizing a mass spectrometry-based profiling system: over-expression of CD36, CD44, CDK9, and PP2A. *Analyst*. 2012;137(21):4921–4933.
22. Jones DS, Irwin CR, Woolfson AD, Djokic J, Adams V. Physicochemical characterization and preliminary in vivo efficacy of bioadhesive, semisolid formulations containing flurbiprofen for the treatment of gingivitis. *J Pharm Sci*. 1999;88(6):592–598.
23. Andrews GP, Donnelly L, Jones DS, et al. Characterization of the rheological, mucoadhesive, and drug release properties of highly structured gel platforms for intravaginal drug delivery. *Biomacromolecules*. 2009;10(9):2427–2435.
24. Baloğlu E, Karavana SY, Hyusein IY, Köse T. Design and formulation of mebeverine HCl semisolid formulations for intraorally administration. *AAPS Pharm Sci Tech*. 2010;11(1):181–188.
25. Chung TW, Wang SS, Tsai WJ. Accelerating thrombolysis with chitosan-coated plasminogen activators encapsulated in poly-(lactide-co-glycolide) (PLGA) nanoparticles. *Biomaterials*. 2008;29(2):228–237.
26. Wang SS, Chou NK, Chung TW. The t-PA-encapsulated PLGA nanoparticles shelled with CS or CS-GRGD alter both permeation through and dissolving patterns of blood clots compared with t-PA solution: An in vitro thrombolysis study. *J Biomed Mater Res A*. 2009; 91(3):753–761.
27. Wang YH, Chung TW, Lai JY, et al. A viscometric method to study the effects of hematocrit of blood and different surfaces of biomaterials on blood clot formation. *J Chin Inst Chem Eng*. 2000;31(1):27–32.
28. Kanazawa KK, Gordon JG. Frequency of a quartz microbalance in contact with a liquid. *Anal Chem*. 1985;57:1770–1771.
29. Lai BF, Zou Y, Brooks DE, Kizhakkedathu JN. The influence of poly-N-[(2,2-dimethyl-1,3-dioxolane)methyl]acrylamide on fibrin polymerization, cross-linking and clot structure. *Biomaterials*. 2010;31(22): 5749–5758.